

THE NATURE OF THE X-RAY BINARIES
IN THE WHIRLPOOL GALAXY/ M51

HONORS THESIS

Presented to the Honors Committee of
Texas State University
in Partial Fulfillment
of the Requirements

for Graduation in the Honors College

by

Luis Bichon III

San Marcos, Texas
May 2018

THE NATURE OF THE X-RAY BINARIES
IN THE WHIRLPOOL GALAXY/ M51

Thesis Supervisor:

Blagoy Rangelov, Ph.D.
Department of Physics

Approved:

Heather C. Galloway, Ph.D.
Dean, Honors College

COPYRIGHT

by

Luis Bichon III

2018

FAIR USE AND AUTHOR'S PERMISSION STATEMENT

Fair Use

This work is protected by the Copyright Laws of the United States (Public Law 94-553, section 107). Consistent with fair use as defined in the Copyright Laws, brief quotations from this material are allowed with proper acknowledgement. Use of this material for financial gain without the author's express written permission is not allowed.

Duplication Permission

(Choose one of the two below and type only it on the page. Remove underline from below your name.)

As the copyright holder of this work I, Luis Bichon III, authorize duplication of this work, in whole or in part, for educational or scholarly purposes only.

OR

As the copyright holder of this work I, Luis Bichon III, refuse permission to copy in excess of the "Fair Use" exemption without my written permission.

DEDICATION

This thesis is dedicated to Jasi Lane Mitchell. Like Atlas to the world you supported me through some of the toughest years of my life. I am happy to say that we succeeded together.

ACKNOWLEDGEMENTS

Throughout my life I have had a few people I consider great mentors. I wish to recognize the two greatest, and their impact on my education. To begin, I would like to express gratitude to Dr. Blagoy Rangelov. You aided me in my undergraduate journey, serving as mentor, a role model, and a friend. With all of your guidance throughout my time at Texas State I achieved many of my goals, and more. I have the utmost respect for you. Another great mentor that I am fortunate enough to have is Dr. Heather Galloway. You have a genuine desire to see your students prosper, and that was paramount to my success. The countless advice you have given me, has opened doors I would have never known existed, and for that I thank you. I aspire to be a great physicist like the both of you someday. I would also like to thank my colleague, and close friend Clint Boldt. You made all of our work, time, and research an amazing experience.

TABLE OF CONTENTS

	Page
ACKNOWLEDGEMENTS	iv
LIST OF TABLES	vi
LIST OF FIGURES	vii
LIST OF ILLUSTRATIONS	viii
ABSTRACT	ix
CHAPTER	
I. INTRODUCTION	1
II. DATA	8
III. METHODOLOGY	10
IV. RESULTS	14
V. CONCLUSION	18
APPENDIX SECTION	20
REFERENCES/LITERATURE CITED.....	23

LIST OF TABLES

Table	Page
1. Sample Data	17
2. Full Data	20

LIST OF FIGURES

Figure	Page
1. Stellar Life Cycle	2
2. X-ray Binary.....	3
3. Messier 51 the “Whirlpool Galaxy”	5
4. Hertzsprung-Russel Diagram	6
5. Transmission vs. Wavelength	8
6. Aperture Photometry	11
7. X-ray Source Locations	13
8. Color Magnitude Diagram 1	15
9. Color Magnitude Diagram 2	16
10. Stellar Classification in M51.....	17

LIST OF ABBREVIATIONS

Abbreviation	Description
ACS	Advanced Camera for Surveys
Be	Be Star
BH	Black Hole
CMD	Color Magnitude Diagram
CXC	Chandra X-Ray Center
DEC, decl	Declination
DS9	SAOImage DS9
FITS	Flexible Image Transport System
HLA	Hubble Legacy Archive
HMXB	High Mass X-Ray Binary
HR	Hertzsprung-Russel
HST	Hubble Space Telescope
LMXB	Low Mass X-Ray Binary
M51	Messier 51
MYR	Million years
NASA	National Aeronautics & Space Administration
NS	Neutron Star
RA	Right Ascension
SG	Super Giant
SNR	Super Nova Remnant
XRB	X-Ray Binary

ABSTRACT

This research consists of the analysis of data from space based observatories such as the Hubble Space Telescope and Chandra X-ray Observatory. The method includes the stellar identification of optical sources in Messier 51 (the Whirlpool Galaxy) found in images from the Hubble Space Telescope. A multi-wavelength analysis (including aperture photometry) is performed on the identified stars, followed by age-dating, and mass estimation. These results are then cross-correlated with the results from preexisting catalogues of X-ray sources. These findings yield a deeper understanding of the nature of the X-ray binaries in the Whirlpool Galaxy and provide greater insight on the X-ray binary formation, and evolution in the galaxy. This knowledge can be generalized to other spiral galaxies much like our own Milky Way.

INTRODUCTION

Over the last few centuries, our knowledge of the universe has increased tremendously thanks to our improved understanding of stellar evolution, the process of star formation, their life, and death. The life of a star follows a particular path that depends mostly on its mass. For instance, when the most massive stars exhaust their fuel, they end their lives with spectacular explosions called supernova remnants (SNRs). The remnants of such stars are very compact objects called neutron stars (NSs) and, if the stellar mass remnant exceeds $3 M_{\odot}$ ¹, black holes (BHs) are formed. X-ray binaries (XRBs) were discovered within the last several decades, and there are still many aspects of the XRB formation and evolution that we do not know.

Stellar life begins inside clouds of gas and dust in space called nebulae. Protostars are born in the nebulae when an accumulation of material begins to collapse in on itself by its own gravity. Eventually nuclear fusion ignites in the core of the protostar and it becomes a main-sequence star. A star will live out most of its existence on the main-sequence primarily fueled by the fusion of hydrogen. A star's life is predominantly determined by the amount of mass it is born with. Massive stars, $M \gtrsim 10 M_{\odot}$, burn their nuclear fuel very fast thus being very bright, but as a result don't live for very long time, ≤ 10 million years, while low mass stars, $\leq 2 M_{\odot}$, can last for billions of years. Once the hydrogen is exhausted the star leaves the main-sequence and becomes a "giant" where it primarily burns helium (see Figure 1). Eventually they will become a BH, NS, or white dwarf depending on its initial mass.

¹ $1 M_{\odot}$ represents 1 solar (sun) mass: $\sim 1.989 \times 10^{30}$ kg

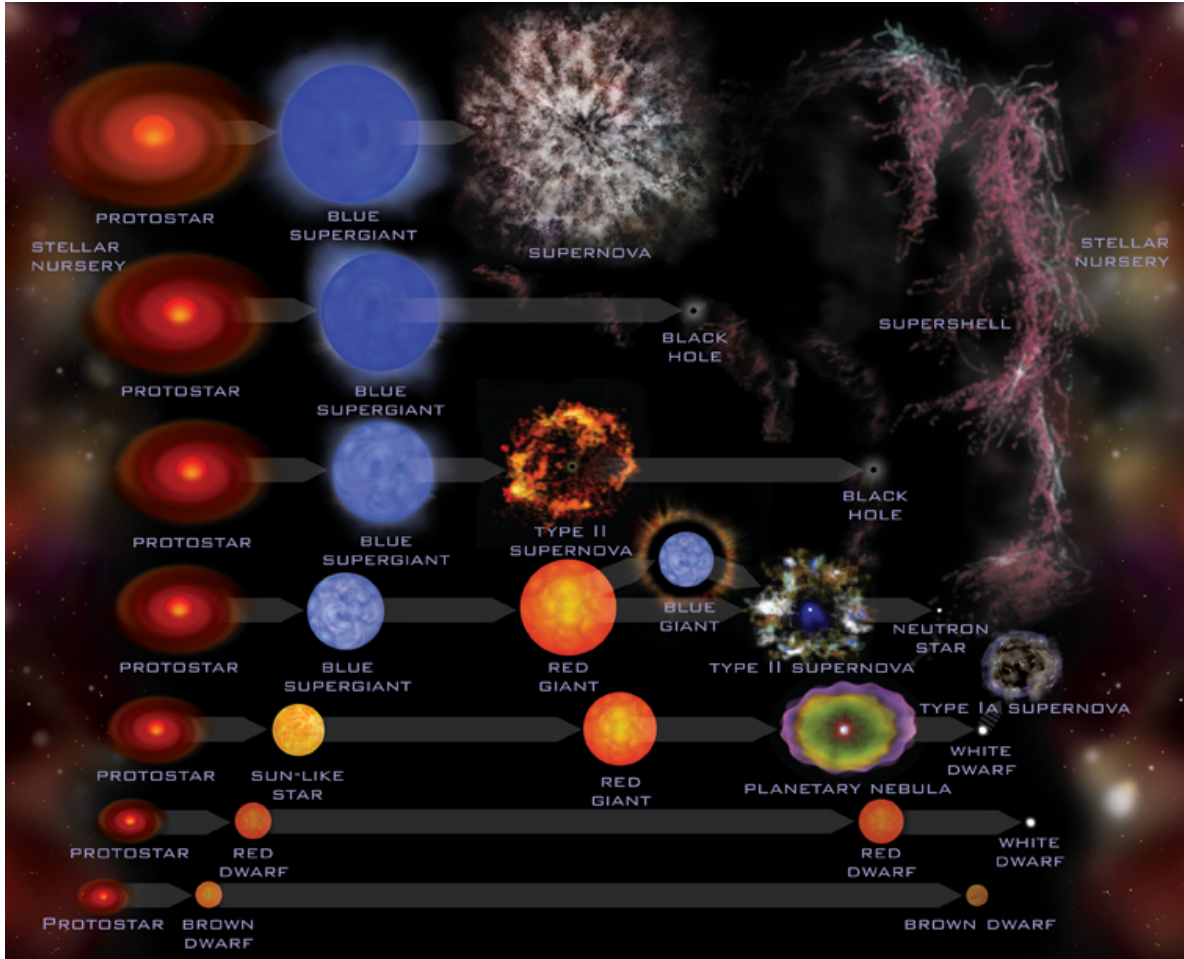


Figure 1: Artistic rendition of the different paths of life a star can take beginning at the bottom with smallest to largest masses up at the top. (Credit: NASA/CXC²)

An XRB is a system of two stars orbiting a common center of mass (Fabbiano 1989, 2006). They consist of one compact star (BH or NS, both known to have very strong gravitational fields) and a companion (main sequence or evolved) star. When the two stars are close enough to each other, a mass transfer occurs from the companion star on to the compact star (see Figure 2). NSs and BHs are known to have very strong gravitational fields. Material from the donor star falls onto the dense accretor/compact

² https://www.nasa.gov/audience/forstudents/9-12/features/stellar_evolution_feat_912.html

object thus releasing gravitational potential energy in the form of X-rays, which is why these systems were originally named XRBs (see Figure 2). There are many subclasses of XRBs, however, they are traditionally classified as low mass XRBs (LMXBs), or a high mass XRBs (HMXBs), based on the companion star. For this thesis we focus only on the HMXB, and leave LMXB for future work (Fabbiano 1989).

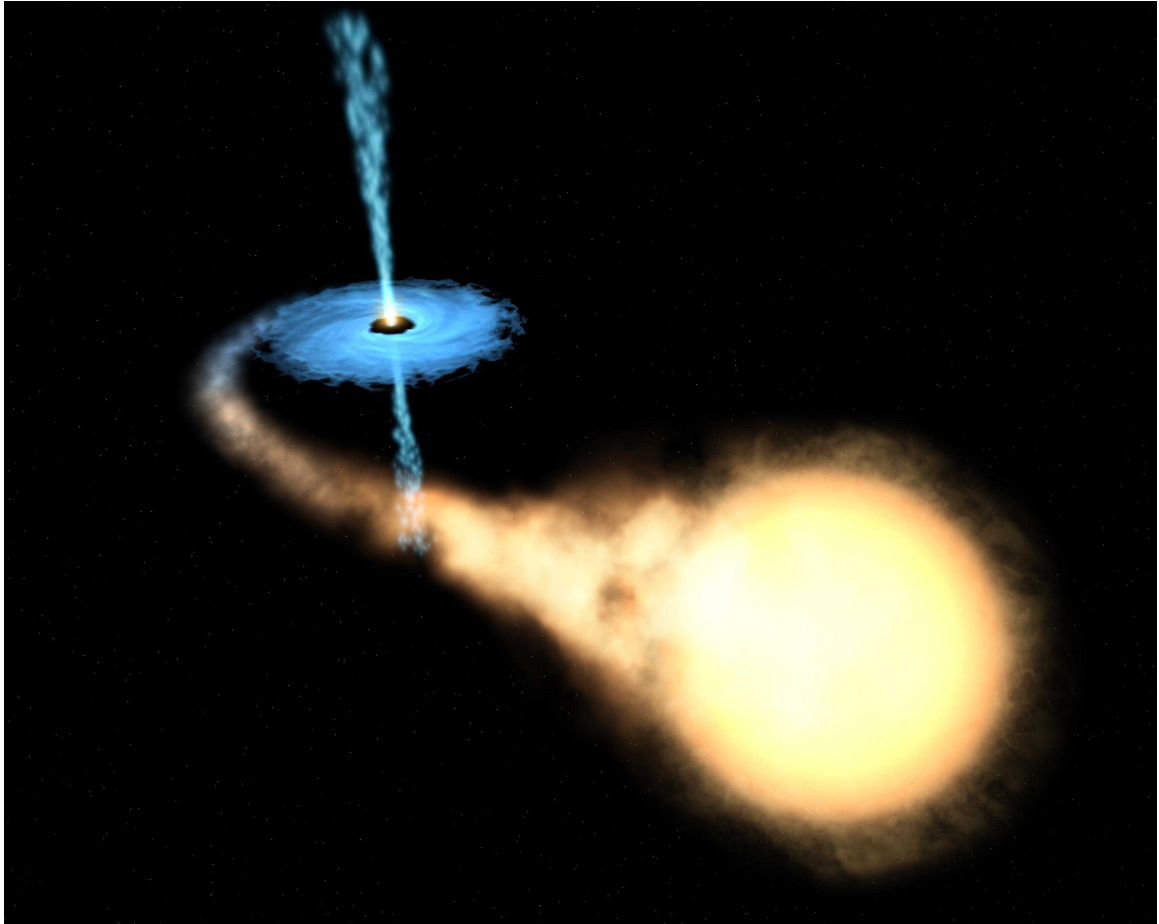


Figure 2: Artistic rendition of an X-ray binary the compact object is “leaching” material from the donor star that is being accreted into a disk thus releasing significant amount of energy by emitting X-rays. (Credit: NASA/CXC³)

³ https://imagine.gsfc.nasa.gov/science/objects/binary_stars1.html

HMXBs can be further divided into two general categories based on the type of donor star: 1) a Be star (Be/XRBs), or 2) a supergiant star (SG/XRBs). Be stars rotate very rapidly, and as a result matter escapes the star and forms an equatorial disk. An orbiting compact object “diving” through the disk of such a star could significantly increase the amount of X-ray emission. Supergiant stars lose a substantial amount of mass through powerful winds. X-rays are produced as the compact object plunges through the stellar wind during its orbit. Outflows from supergiants can contain large clumps of material, which can result in rapid changes of the X-ray emission. Supergiants are evolved very massive stars, that, depending on the binary parameters, can fill their Roche-Lobes, thus making it easier for material to be transferred onto the compact object. The Roche-Lobe is a tear-shaped equipotential surfaces around the stars where the objects gravity dominates. In Roche-Lobe overflow, material beyond that region can “feel” the gravitational pull of the compact object and be easily accreted on to it⁴.

⁴ http://www-astro.physics.ox.ac.uk/~podsi/lec_c1_4_c.pdf



Figure 3: This famous photo is the sharpest image of Messier 51 to date, taken with the Advanced Camera for Surveys (ACS) on board of the Hubble Space Telescope. M51 is approximately 7.4×10^6 parsecs (or 2.3×10^{20} kilometers) away. (Credit: NASA HST⁵)

Messier 51 (M51), famously known as the “Whirlpool Galaxy,” is an interacting spiral galaxy (two galaxies currently in the process of colliding [1, 2]). M51 is an ideal galaxy to study because it is a “face-on” galaxy (it has a relatively low inclination angle), which makes it possible to detect sources, and identify their locations within the galaxy (see Figure 3). Another reason this galaxy is ideal is that it is a spiral galaxy (like the Milky Way), and approximately ~ 0.3 times the mass^{6,7}.

⁵ http://hubblesite.org/image/1677/news_release/2005-12

⁶ https://www.nasa.gov/mission_pages/chandra/multimedia/spiral-galaxy-m51.html

⁷ <https://freestarcharts.com/messier-51>

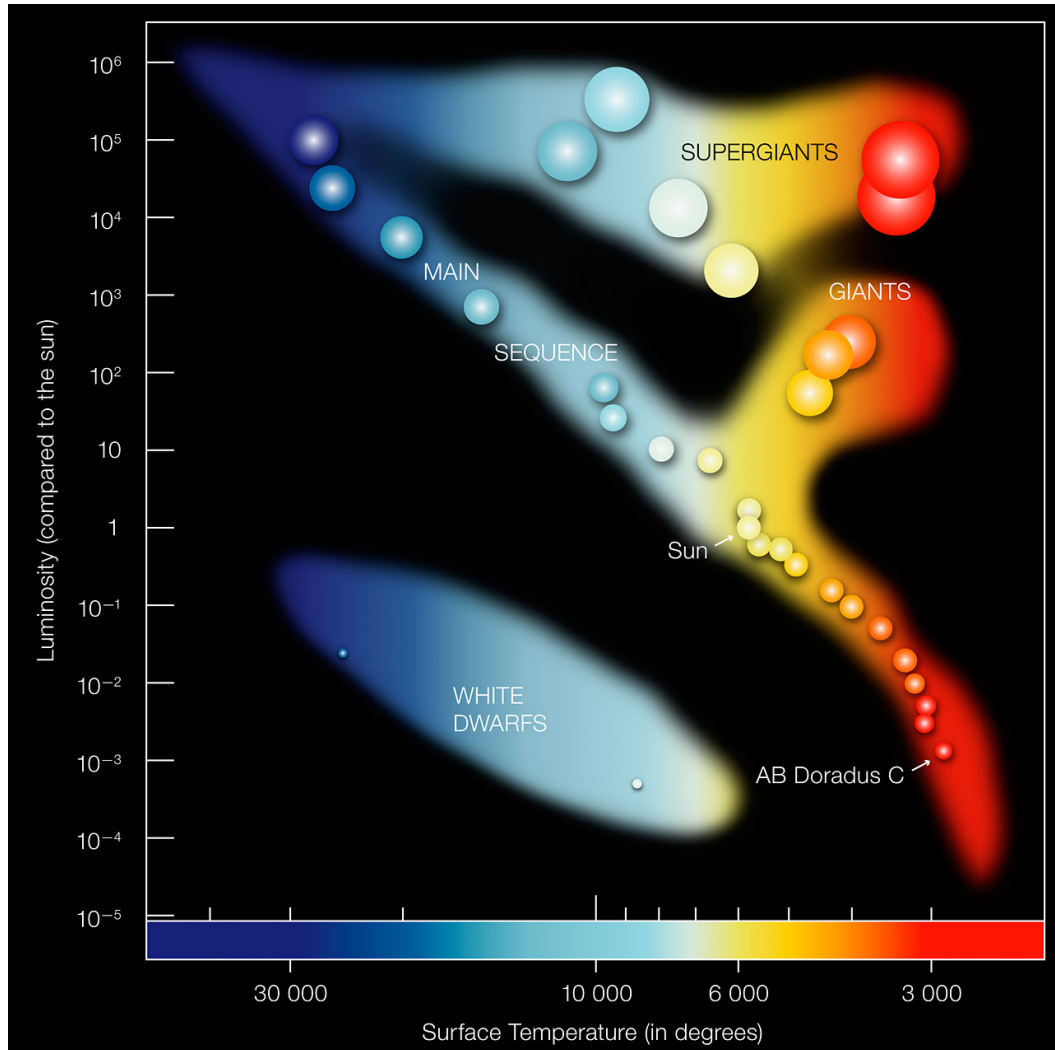


Figure 4: An example of a Hertzsprung-Russel Diagram. This type of Hertzsprung Russel Diagram is a Luminosity vs. Surface Temperature graph. Note: we may typically see spectral type associated with the temperature on the x-axis, however, the evolutionary stages are still present (e.g. White Dwarfs, Main Sequence). (Credit: Wikipedia⁸)

The primary goal of this thesis is to identify all X-ray sources, and create an X-ray catalog of sources that have optical counterparts. This allows us to study the nature of the XRBs within a spiral galaxy much like our own Milky Way, and compare the results to other spiral galaxies. In astronomy, we use a tool called a Hertzsprung-Russel (HR)

⁸ <https://www.eso.org/public/images/eso0728c/>

Diagram. This is essentially a chart where stars are plotted with luminosity vs. temperature (or color), and serves as a powerful tool in the classification of stars (see Figure 4)⁹.

⁹ <http://astronomy.swin.edu.au/cosmos/H/Hertzprung-Russell+Diagram>

DATA

The Hubble Space Telescope (HST) is a conglomerate of different instruments all with the purpose of gathering information about stars, star clusters, galaxies, and other celestial objects. These instruments allow us to study the Universe in ultraviolet, visible, and near infrared electromagnetic spectrum. We utilize one of these instruments, the Advanced Camera for Surveys (ACS), which measures light in the visible spectrum. The filters we use are the F435W (blue), F555W (green or “visible”), and F814W (red). The filter names also correspond to the peak wavelength in nanometers, and the reason these three are chosen is because they span the entirety of the visible light spectrum (with ranges between $\sim 4000 \text{ \AA}$ and $\sim 7000 \text{ \AA}$; see Figure 5).

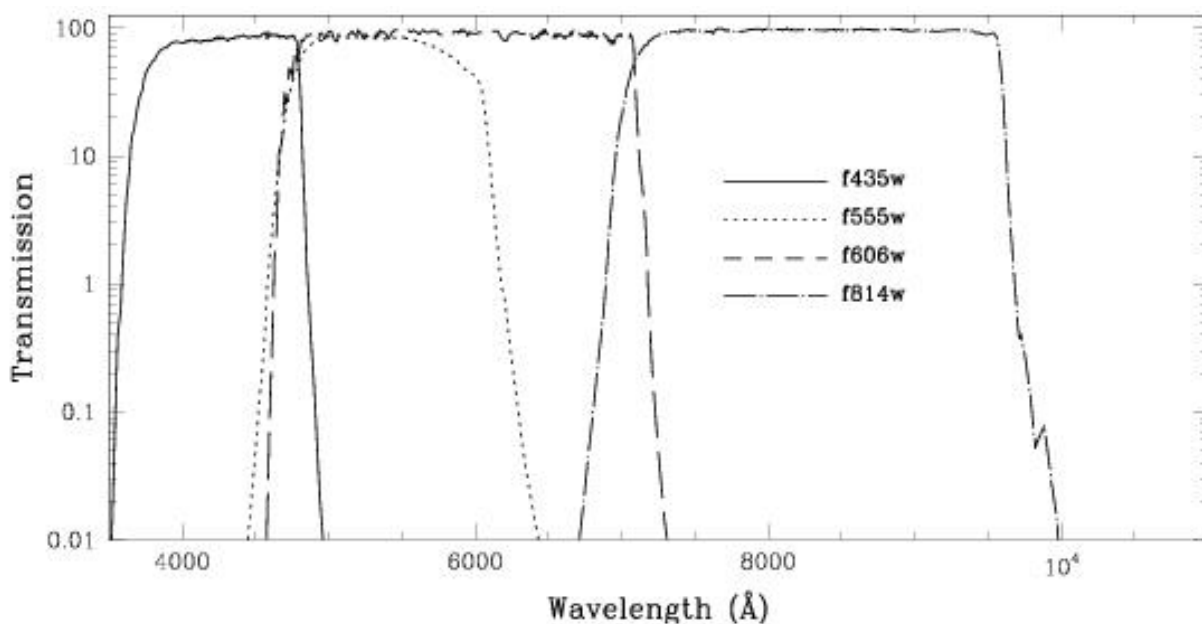


Figure 5: In the case of this image the Transmission (How much incoming flux/light is allowed through) vs. the Wavelength in angstroms or 1×10^{-10} meters. Note: The F606W filter is not used in our research. (Credit: Space Telescope Science Institute¹⁰)

¹⁰ http://www.stsci.edu/hst/acs/documents/handbooks/current/c05_imaging2.html

In addition to the HST, we also utilize the Chandra X-ray Observatory (Chandra). Both instruments are essential to study the nature of the X-ray binaries. The distance from where we are in the Milky Way to M51 is far too large for us to have the ability to resolve the binary star, which is also very faint in the optical and can only be detected in X-rays. This issue is remedied by locating sources where X-rays are being emitted, and then superimposing their locations onto an image with visible sources. Any X-ray source without an optical counterpart are a topic of a different study and will not be discussed in this thesis.

METHODOLOGY

Flexible Image Transport System (FITS) is an open standard digital file format used for storage and processing of scientific data. FITS is the most commonly used digital file format in astronomy. Unlike many image formats, FITS is designed to store scientific data sets consisting of multidimensional arrays (images) and 2-dimensional tables organized into rows and columns of information. The FITS format includes an image metadata stored in a human-readable ASCII header, which includes description of photometric and spatial calibration information, together with image origin metadata, and other relevant information¹¹.

We acquired the data from the Hubble Legacy Archive¹². We choose FITS files created by the Hubble Heritage Project, which come calibrated, ready for scientific analysis. Specifically, we use 3 filters in the optical band with peak wavelengths: 435 nm (B band), 555 nm (V band), and 814 nm (I band). These wavelengths give us a broad range that contains the visible spectrum. The images cover the same part of the sky, so we examined the *V* filter file for constructing the pipeline, or general visual inspection.

We construct a versatile pipeline, which enables us to apply it to any FITS file, allowing for data analysis of any celestial object. We analyzed data by performing a technique called aperture photometry (Figure 6), which is a method of measuring the flux of electromagnetic radiation, or light intensity, for a given astronomical object. The focus of this research is using aperture photometry to study the stellar population (which appear as point like sources in the data). We start by creating an aperture (ring) around the source, and then we sum all pixel values to calculate the flux in the aperture. There are

¹¹ https://fits.gsfc.nasa.gov/standard30/fits_standard30.pdf

¹² <http://hla.stsci.edu/>

several factors that could introduce error to our measurements. These include sources located in a region with high extinction (e.g., interstellar clouds between the source and the observer that will “dim” the light), or regions with a non-uniform background. To account for this, we take an area surrounding the source (an annulus), and find the average flux value within that region. We can then subtract the value from the source intensity measured in the aperture, taking into account the different areas of the aperture and annulus (Figure 6). All of the aperture photometry, and the creation of the pipeline is done with the utilization of the Python programming language.

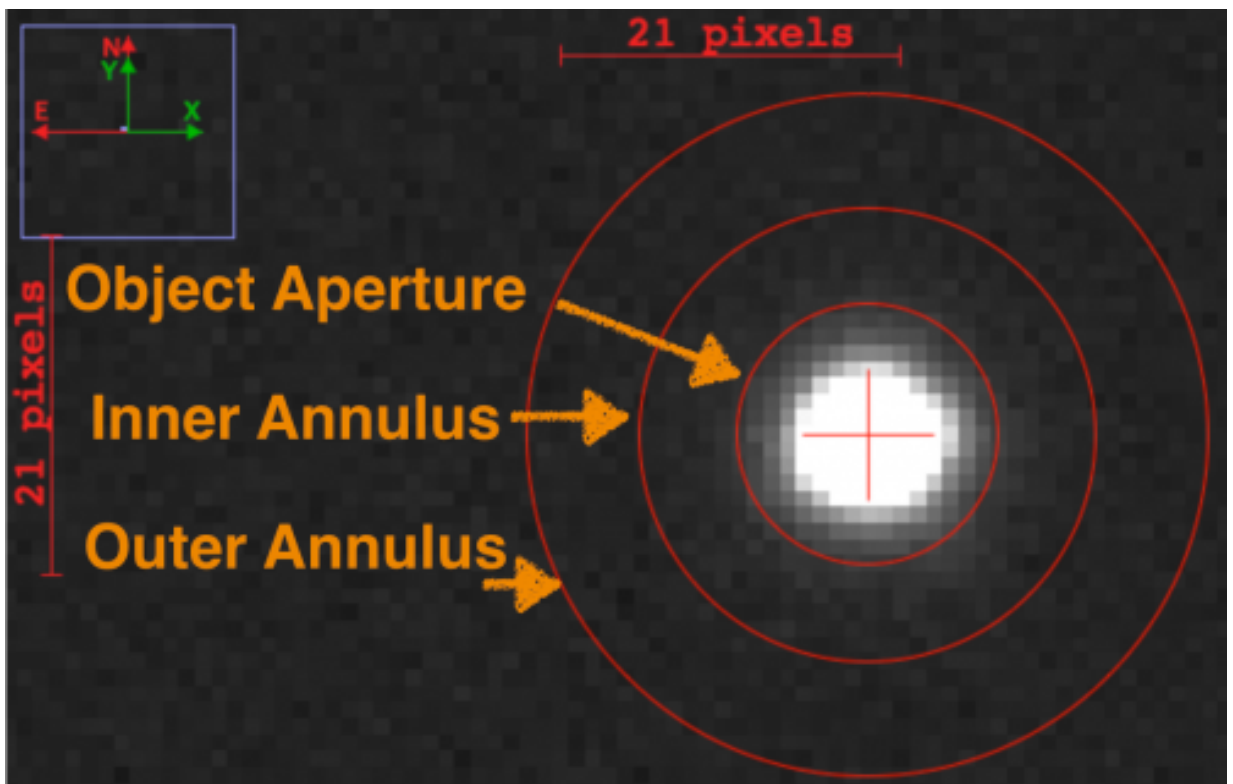


Figure 6: Located at the center of the apertures (rings) is the source (white pixels). Two annuli are generated (inner and outer), and an average value is calculated within the area formed by both annuli. That average value is then subtracted from the value of the source in order to generate a corrected magnitude for our optical source. (Credit: Astrobites¹³)

¹³ https://astrobites.org/wp-content/uploads/2016/04/aij_aperture-e1460731340188.png

The initial goal of the pipeline methodology is to locate all point sources (stars) in the data. We use the following parameters: aperture: $r = 3$ pixels; inner annulus: $r = 8$ pixels; outer annulus: $r = 12$ pixels. A sample image produced with apertures can be seen in Figure 6 using the parameters previously mentioned. A final catalog of $\sim 93,000$ point-like sources, is then created. A majority of those are the bright stars in M51, but for the purpose of this project we will focus only on those that coincide with an X-ray source.

In order to find optical counterparts to the XRBs in M51, we first need to perform astrometric corrections (match the X-ray and optical coordinate systems). We used an already existing catalog of XRBs in M51 containing the celestial coordinates (R.A. and decl.) for each X-ray source. We first identified the optical counterparts to 10 X-ray sources in the outer regions of the V-band image. None of these sources are located within the main body of the galaxy, and we verified that these are background or foreground sources. The comparison between the X-ray and optical coordinates for these 10 sources gives a mean shift of $0.72''$ ($0.04''$ in R.A. and $0.72''$ in decl.), and a standard deviation (i.e., 1σ positional uncertainties) of $\approx 0.5''$ (which is comparable to the Chandra positional uncertainty).

Figure 7 shows the distribution of X-ray sources in M51, however, some of the sources provided have no optical counterpart. When we visually inspect the image if no counterpart is within a $0.5''$ radius we choose to remove that source reducing the number of XRB candidates. We are left with a list of 90 XRB candidates for which we extract the fluxes in all three HST bands (see Appendix – Table 1).

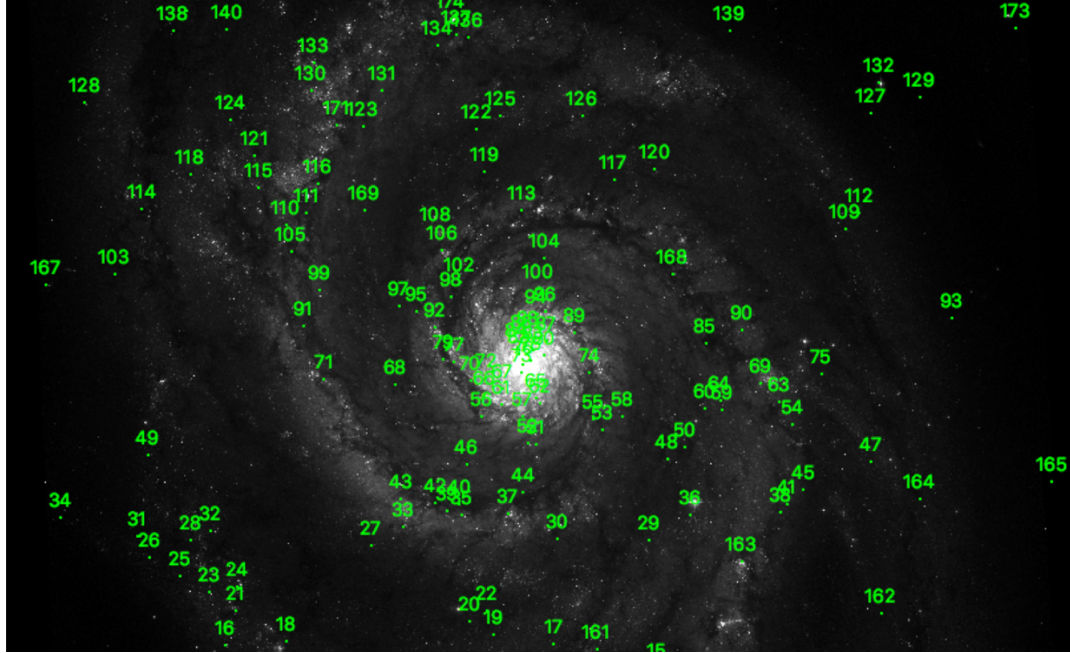


Figure 7: A cropped image of M51 centered at the nucleus, produced in DS9 “an astronomical imaging and data visualization application”¹⁴; using the 555 nm filter. Each number represents the ID number of an X-ray source. Note: not all X-ray sources are used due to the lack of optical counterparts.

To calculate the observed magnitudes for each source we use the following equation:

$$m = -2.5 \log(\text{PHOTFLAM}) - 5 \log(\text{PHOTPLAM}) - 2.408 - 2.5 \log(\text{NET}),$$

where PHOTFLAM is a calibration constant (inverse sensitivity in units of $\text{erg}/\text{cm}^2/\text{s}/\text{\AA}$), PHOTPLAM is the peak wavelength of the filter, and NET is the background-subtracted count rate of the source. The above equation is generalized to be applied any filter (B, V, and I). The corresponding magnitude error can be described by:

$$m_{\text{err}} = 1.0857 \left(\frac{\text{NET}_{\text{err}}}{\text{NET}} \right)$$

where NET_{err} is the background-subtracted count rate error¹⁵.

¹⁴ <http://ds9.si.edu/site/Home.html>

¹⁵ <http://www.stsci.edu/hst/acs/analysis/zeropoints>

RESULTS

To determine the nature of the X-ray source counterparts in the optical data, we use theoretical models of stellar evolution. We compare our measurements to the theoretical isochrones (a curve on an HR diagram corresponding to a population of stars that have the same age, but different masses). This allows us to determine the spectral classification, age, and mass of each donor star. We used the Padova database of stellar evolutionary tracks and isochrones¹⁶.

The isochrones are provided in absolute magnitudes. To be able to directly compare them to our measurements, we converted the isochrones to apparent magnitudes using the following relationship:

$$m = M + 5(\log(d) - 1)$$

where, M is the absolute magnitude, and d is the distance to M51. We used $d = 7.4 \times 10^6$ pc = 2.3×10^{20} km [ref]. An apparent magnitude is the magnitude of the celestial object when viewed from Earth, and an absolute magnitude is the normalized magnitude if the object is placed to be 10 parsecs away.

We created two color-magnitude diagrams (CMDs; the observational version of the HR diagram) to better constrain the stellar properties (Figures 8 and 9). We compare our data to four isochrones ranging from very young ages (5 Myr) to intermediate ages (100 Myr). These age ranges cover the evolution of very massive stars. Beyond ~100 Myr, all B-type (Be) stars reached the end of their lifetimes, while O-type stars (Supergiants) would not last more than ~10 Myr. Figures 8 and 9 show the difference in

¹⁶ <http://pleiadi.pd.astro.it/>

the classes of HMXBs, with the dashed line, at $V = 23.3$ ($M_V = -6$), illustrating the approximate separation between O- and B-type stars.

Color Magnitude Diagram 1

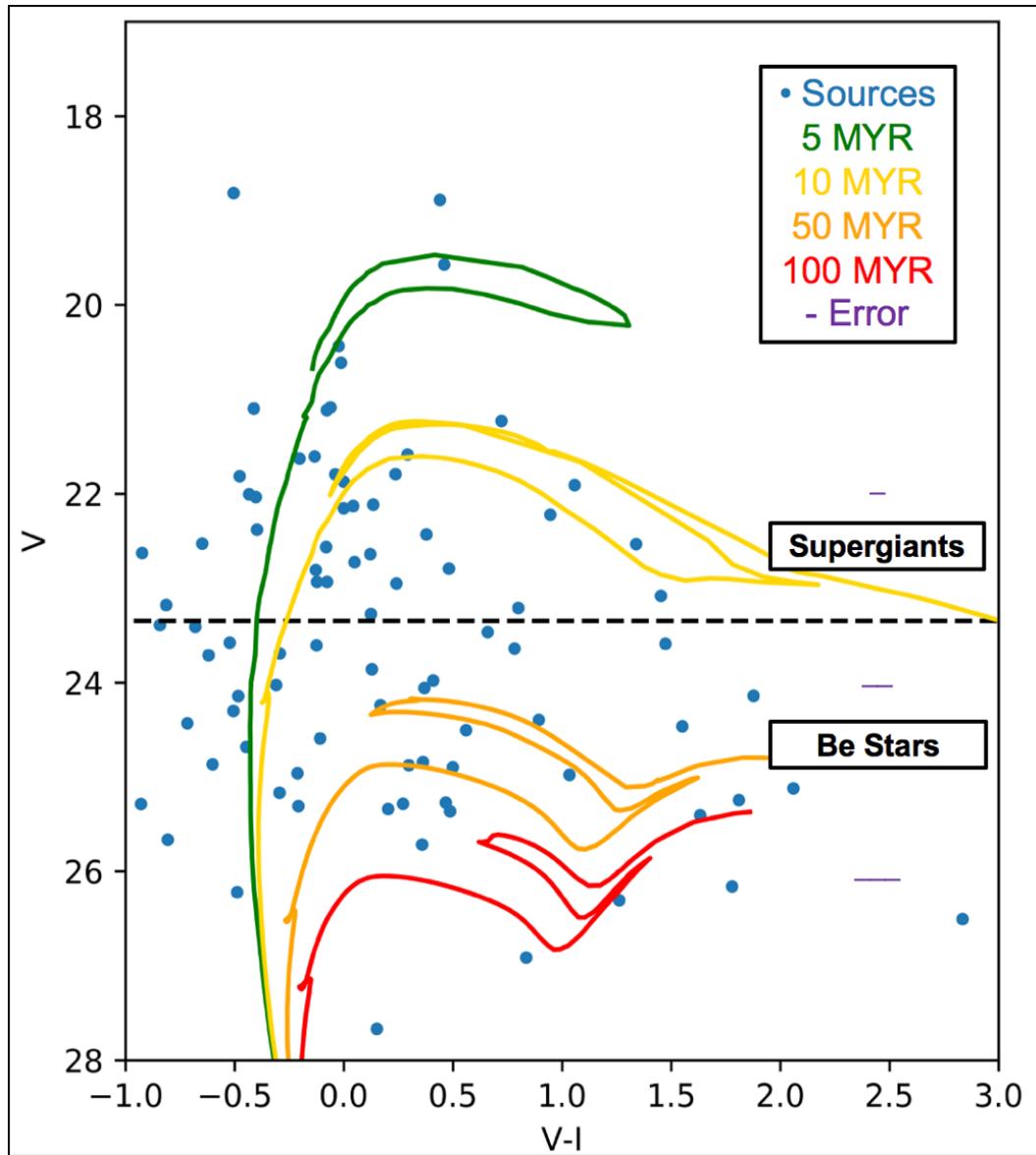


Figure 8: A color-magnitude diagram V magnitude vs. V-I magnitude. Superimposed are the 5 Myr, 10 Myr, 50 Myr, & 100 Myr isochrones. The dashed line represents the cutoff between Supergiants, and Be stars; with the sources above representing the Supergiants, and the sources below representing the Be stars. The average errors are plotted for V magnitudes ranging from V magnitude: 19 to 21, 21 to 23, 23 to 25, and 25 to 27. These averages are plotted on the sides of the diagram to reduce clutter.

Color Magnitude Diagram 2

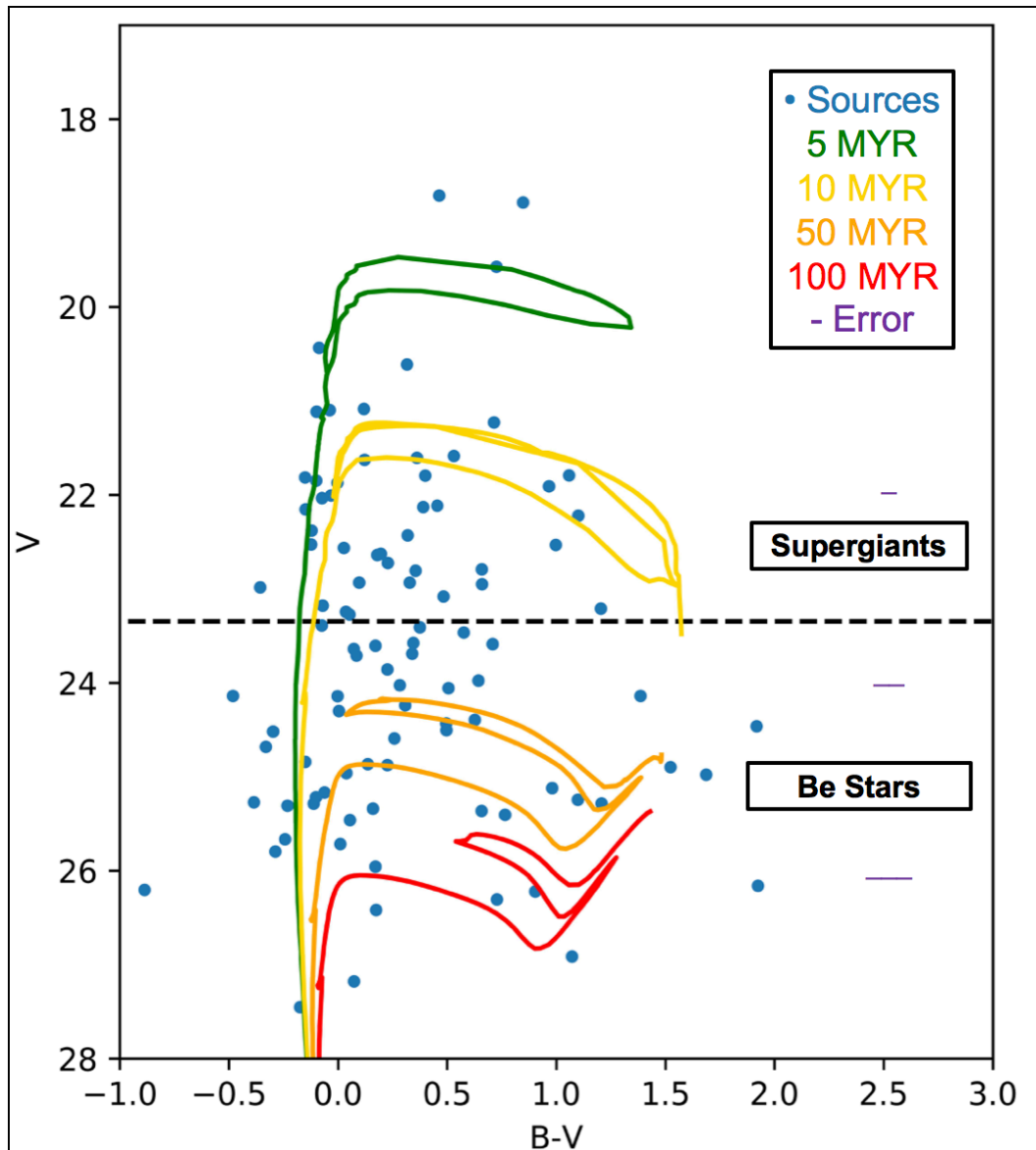


Figure 9: A color-magnitude diagram V magnitude vs. B-V magnitude. Superimposed are the 5 Myr, 10 Myr, 50 Myr, & 100 Myr isochrones. The dashed line represents the cutoff between Supergiants, and Be stars; with the sources above representing the Supergiants, and the sources below representing the Be stars. The average errors are plotted for V magnitudes ranging from V magnitude: 19 to 21, 21 to 23, 23 to 25, and 25 to 27. These averages are plotted on the sides of the diagram to reduce clutter.

Table 1 includes the first five HMXB candidates in the catalog. The first column represents the X-ray ID number from the 177 sources initially used. The HMXB type classification is listed in the last column.

Table 1: High Mass X-ray Binary Magnitudes with Stellar Classification

XID	RA	DEC	B Mag	Error B	V Mag	Error V	I Mag	Error I	Classification
4	202.5269856	47.14298923	21.94232978	0.001721546	21.22780276	0.001913238	20.50592198	0.000720966	Supergiant
5	202.4796515	47.14450375	20.92604703	0.001072476	20.61070101	0.00157668	20.62415063	0.001063928	Supergiant
8	202.4099793	47.15451243	24.69020901	0.006533601	24.84079316	0.003705973	24.47794879	0.005956164	Be Star
11	202.4791209	47.15630884	26.38508356	0.017518166	25.9119262	0.003864325	25.21529432	0.008299836	Be Star

Once the candidate donor stars are categorized as Supergiants or Be stars, we can plot their location throughout the galaxy. Figure 10 shows V-band image of M51 with Be stars and Supergiants encircled by green and red circles, respectively.

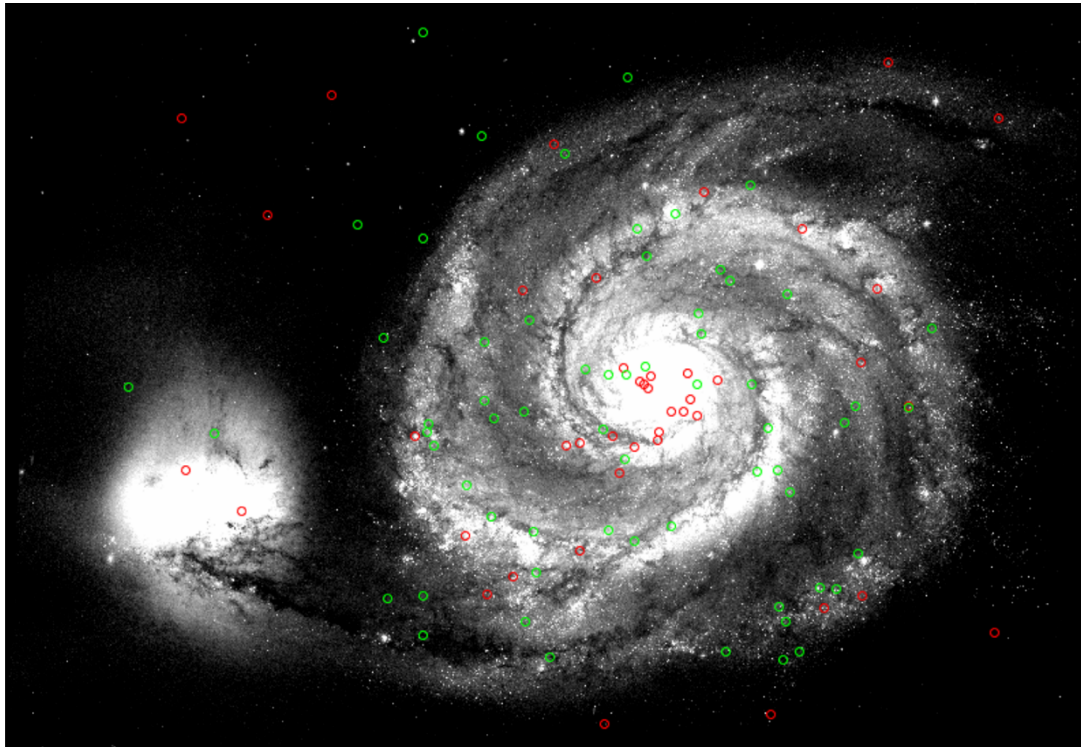


Figure 10: An image of M51 created in DS9 with the locations of Be Stars (green apertures), and Supergiants (red apertures) superimposed on the image.

CONCLUSION

We have performed a multi-wavelength study of the X-ray sources in the Whirlpool Galaxy. We used X-ray information from the Chandra, and optical data (in three filters) from the HST. We used CMDs to determine the ages of the HMXB donor star candidates. Our main conclusions are:

- The Whirlpool Galaxy contains a mixed population of donor star candidates (Supergiants and Be stars). We also see that large number of stars fall in areas of the CMDs corresponding to evolved objects (located to the right of the main sequence). This indicates that in many of the HMXBs, the accretion is happening through Roche-Lobe overflow (Fabbiano 2006).
- From the spatial distribution of donor stars shown on Figure 8, it is clear that, on average, Supergiants are located closer to the spiral arms than Be stars. This is to be expected given that 1) star formation is taking place primarily in the spiral arms, and 2) Supergiants have shorter lifespans, and, hence, less time to travel away from their birth sites.
- Out of the 177 X-ray sources located within the main body of M51, only 90 sources (51%) have an optical counterpart. This suggests that the potential donor star is below the detection limit of the HST, which, at the distance to M51, corresponds to A- or later type stars. Sources lacking a visible counterpart are then likely to be Low Mass X-Ray Binaries.

This study can be further expanded on by performing a similar analysis on other galaxies with similar properties (e.g., low inclination angle, spiral arms, interacting) and comparing the results. Although the work in this thesis provide us with understanding of

the nature of X-ray sources in the Whirlpool Galaxy, increasing the number of studies will help us understand the formation and evolution of XRBs in the universe. I will expand upon my results in future endeavors.

APPENDIX

Table A1: X-ray source Catalog

XID	RA	DEC	B Mag	Error B	V Mag	Error V	I Mag	Error I	Classification
4	202.52699	47.14299	21.942	0.002	21.228	0.002	20.506	0.001	Super Giant
5	202.47965	47.14450	20.926	0.001	20.611	0.002	20.624	0.001	Super Giant
8	202.40998	47.15451	24.690	0.007	24.841	0.004	24.478	0.006	Be Star
11	202.47912	47.15631	26.385	0.018	25.912	0.004	25.215	0.008	Be Star
12	202.47494	47.15650	25.389	0.010	25.555	0.004	26.241	0.024	Be Star
13	202.39569	47.15961	22.403	0.002	22.527	0.003	23.176	0.005	Super Giant
14	202.44781	47.16130	19.736	0.001	18.888	0.001	18.448	0.000	Super Giant
15	202.51884	47.16376	21.016	0.001	21.115	0.002	21.193	0.001	Super Giant
16	202.46478	47.16398	22.817	0.003	22.638	0.003	22.517	0.002	Super Giant
17	202.50882	47.16422	23.609	0.004	22.949	0.003	22.708	0.003	Super Giant
18	202.47467	47.16498	23.314	0.003	23.389	0.003	24.232	0.009	Be Star
20	202.51711	47.16770	24.561	0.006	24.056	0.004	23.687	0.004	Be Star
21	202.47582	47.16765	24.321	0.005	23.932	0.004	24.141	0.006	Be Star
22	202.52141	47.16971	25.566	0.011	25.893	0.004	26.792	0.036	Be Star
23	202.51678	47.17040	22.567	0.002	22.113	0.002	21.978	0.002	Super Giant
24	202.52630	47.17148	25.316	0.010	26.202	0.003	N/A	N/A	Be Star
26	202.49483	47.17503	24.998	0.007	24.961	0.005	25.173	0.010	Be Star
27	202.52445	47.17558	25.525	0.010	24.140	0.003	22.263	0.001	Be Star
28	202.44914	47.17554	24.849	0.007	24.591	0.004	24.701	0.008	Be Star
31	202.52112	47.17666	27.985	0.046	26.913	0.005	26.078	0.012	Be Star
32	202.48956	47.17706	N/A	N/A	27.666	0.004	27.515	0.048	Be Star
33	202.54599	47.17811	23.334	0.003	23.327	0.002	23.931	0.007	Super Giant
34	202.47984	47.17844	21.963	0.002	21.603	0.002	21.737	0.002	Super Giant
35	202.44224	47.17841	25.099	0.009	24.874	0.002	24.576	0.008	Be Star
38	202.48227	47.17881	24.711	0.007	23.890	0.003	22.721	0.002	Be Star
39	202.48026	47.17959	24.649	0.007	24.684	0.003	24.478	0.007	Be Star
43	202.46981	47.18098	26.127	0.022	25.956	0.002	N/A	N/A	Be Star
44	202.42380	47.18127	28.060	0.064	29.146	0.003	N/A	N/A	Be Star
45	202.47912	47.18404	27.278	0.033	27.452	0.004	N/A	N/A	Be Star
48	202.53155	47.18505	24.114	0.005	23.804	0.003	24.040	0.006	Be Star
49	202.44325	47.18595	25.725	0.011	25.715	0.005	25.357	0.009	Be Star
50	202.46763	47.18622	24.544	0.006	24.238	0.003	24.070	0.005	Be Star
52	202.45670	47.18789	21.202	0.001	21.084	0.002	21.146	0.001	Super Giant
53	202.42544	47.18855	N/A	N/A	26.151	0.003	24.535	0.005	Be Star
54	202.45815	47.18902	23.259	0.003	22.931	0.003	23.055	0.004	Super Giant
55	202.47669	47.18946	N/A	N/A	28.418	0.003	N/A	N/A	Be Star
56	202.46993	47.18939	N/A	N/A	25.684	0.002	24.473	0.007	Be Star
57	202.45345	47.18937	26.380	0.024	24.462	0.002	22.911	0.002	Be Star

59	202.43990	47.19031	25.565	0.011	25.686	0.003	25.686	0.015	Be Star
61	202.46707	47.19089	22.952	0.003	22.724	0.002	22.676	0.003	Super Giant
66	202.47311	47.19257	22.004	0.002	22.153	0.001	22.153	0.002	Super Giant
69	202.47842	47.19342	23.792	0.004	23.709	0.002	24.329	0.009	Be Star
71	202.47585	47.19365	24.082	0.005	23.857	0.002	23.728	0.005	Be Star
72	202.47003	47.19434	22.849	0.003	21.791	0.001	21.554	0.002	Super Giant
77	202.46842	47.19566	21.747	0.002	21.626	0.002	21.829	0.002	Super Giant
79	202.46637	47.19622	24.347	0.006	24.700	0.002	N/A	N/A	Be Star
83	202.47081	47.19718	22.519	0.002	22.130	0.001	22.087	0.002	Super Giant
84	202.43975	47.19753	22.115	0.002	21.584	0.001	21.293	0.001	Super Giant
85	202.47004	47.19798	25.174	0.008	25.286	0.003	26.215	0.026	Be Star
88	202.46132	47.19870	22.627	0.003	22.983	0.001	24.675	0.018	Super Giant
90	202.50590	47.19948	27.124	0.038	26.221	0.003	26.709	0.038	Be Star
91	202.48429	47.19941	25.116	0.008	25.218	0.003	N/A	N/A	Be Star
92	202.39912	47.20033	22.822	0.003	22.627	0.002	23.551	0.007	Super Giant
94	202.48735	47.20106	23.658	0.005	24.140	0.001	N/A	N/A	Be Star
95	202.46602	47.20108	24.041	0.005	23.465	0.003	22.806	0.002	Be Star
96	202.49017	47.20176	22.875	0.003	21.908	0.001	20.851	0.001	Super Giant
97	202.48165	47.20276	23.323	0.003	23.272	0.003	23.148	0.003	Super Giant
99	202.46724	47.20360	24.885	0.008	25.271	0.003	24.804	0.008	Be Star
102	202.53704	47.20527	24.999	0.008	24.864	0.003	25.466	0.016	Be Star
104	202.50796	47.20787	25.508	0.011	25.796	0.003	N/A	N/A	Be Star
105	202.48316	47.20797	27.911	0.062	N/A	N/A	25.521	0.007	Super Giant
106	202.36102	47.20967	23.278	0.004	23.243	0.002	N/A	N/A	Super Giant
108	202.41669	47.21027	21.973	0.002	22.006	0.002	22.441	0.003	Super Giant
112	202.47005	47.21245	23.106	0.003	23.177	0.003	23.991	0.007	Super Giant
114	202.51334	47.21489	24.219	0.005	24.517	0.004	25.709	0.021	Be Star
115	202.50364	47.21537	25.001	0.008	24.503	0.003	23.943	0.004	Be Star
116	202.45484	47.21579	24.349	0.006	24.680	0.003	25.128	0.012	Be Star
117	202.52457	47.21636	26.590	0.020	26.417	0.004	28.045	0.102	Be Star
118	202.47610	47.21677	26.662	0.022	24.976	0.004	23.942	0.003	Be Star
119	202.44813	47.21697	N/A	N/A	26.503	0.004	23.668	0.002	Be Star
120	202.51410	47.21849	24.413	0.006	23.209	0.003	22.411	0.002	Super Giant
121	202.47757	47.22148	22.257	0.002	22.378	0.002	22.777	0.003	Super Giant
122	202.49620	47.22180	26.490	0.018	25.283	0.004	25.012	0.008	Be Star
124	202.47352	47.22294	22.747	0.003	22.429	0.003	22.051	0.002	Super Giant
125	202.45999	47.22300	25.022	0.008	24.395	0.003	23.502	0.003	Be Star
127	202.54203	47.22443	23.710	0.004	23.639	0.005	22.857	0.002	Be Star
131	202.41123	47.22673	25.513	0.011	25.459	0.003	26.605	0.038	Be Star
134	202.58748	47.23142	28.083	0.071	26.159	0.003	24.380	0.004	Be Star
136	202.48083	47.23200	26.019	0.014	25.362	0.004	24.875	0.007	Be Star
138	202.43578	47.23244	24.295	0.005	23.587	0.004	22.113	0.001	Be Star
139	202.51859	47.23260	25.103	0.008	25.166	0.005	25.461	0.012	Be Star

140	202.52512	47.23466	N/A	N/A	28.867	0.004	26.261	0.013	Be Star
143	202.45891	47.23879	26.101	0.013	25.120	0.005	23.060	0.001	Be Star
144	202.47423	47.24215	25.498	0.010	25.339	0.005	25.137	0.009	Be Star
155	202.48775	47.26585	23.322	0.003	22.221	0.002	21.275	0.001	Super Giant
161	202.41090	47.16734	24.181	0.005	25.045	0.003	27.446	0.090	Be Star
163	202.40450	47.18021	19.277	0.001	18.813	0.001	19.318	0.001	Super Giant
168	202.49587	47.21237	22.015	0.002	22.081	0.002	22.473	0.003	Super Giant
171	202.58156	47.22602	24.307	0.006	24.026	0.002	24.336	0.008	Be Star
174	202.40334	47.24701	21.746	0.002	21.847	0.001	22.937	0.005	Super Giant

Note: For some of the sources it was necessary to omit their value due to lack of data in one or more of its respective filters. This reduces the amount of “complete” sources to ~90. Included in the table is the source with ID number, apparent magnitude in each filter (with error), and stellar classification.

REFERENCES

Fabbiano G., 1989, *ARA&A*, 27, 87

Fabbiano, G. 2006, *ARA&A*, 44, 323